AD-A119 075 CASE WESTERN RESERVE UNIV CLEVELAND OH DEPT OF MACROM--ETC F/G 11/9
STRESS RELATED SURFACE TENSION EFFECTS IN HARD ELASTIC POLYMERS--ETC(U)
AUG 82 K WALTON, A MOET, E BAER N00014-75-C-0795
UNCLASSIFIED TR-13 NL

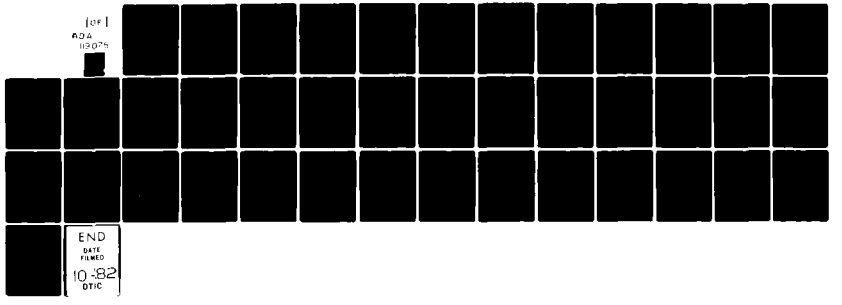

END
DATE FILMED
10-82
DTIC

AD A119075

SECURITY CLASSIFICATION OF THIS PAGE (When Data Entered)

REPORT DOCUMENTATION PAGE

READ INSTRUCTIONS BEFORE COMPLETING FORM

1. REPORT NUMBER: Technical Report #13	2. GOVT ACCESSION NO.: AD-A119075
3. RECIPIENT'S CATALOG NUMBER:	
4. TITLE (and Subtitle): STRESS RELATED SURFACE TENSION EFFECTS IN HARD ELASTIC POLYMERS	5. TYPE OF REPORT & PERIOD COVERED: Technical Report Interim
	6. PERFORMING ORG. REPORT NUMBER:
7. AUTHOR(s): Kim Walton, Abdelsamie Moet and Eric Baer	8. CONTRACT OR GRANT NUMBER(s): N00014-75-C-0795
9. PERFORMING ORGANIZATION NAME AND ADDRESS: Department of Macromolecular Science, Case Western Reserve University, Cleveland, Ohio 44106	10. PROGRAM ELEMENT, PROJECT, TASK AREA & WORK UNIT NUMBERS:
11. CONTROLLING OFFICE NAME AND ADDRESS: Office of Naval Research (Code 472), Arlington, Virginia 22217	12. REPORT DATE: August 19, 1982
	13. NUMBER OF PAGES:
14. MONITORING AGENCY NAME & ADDRESS (if different from Controlling Office)	15. SECURITY CLASS. (of this report): Unclassified
	15a. DECLASSIFICATION/DOWNGRADING SCHEDULE:

16. DISTRIBUTION STATEMENT (of this Report)

Approved for public release; distribution unlimited. Reproduction in whole or in part is permitted for any purpose of the United States Government.

17. DISTRIBUTION STATEMENT (of the abstract entered in Block 20, if different from Report)

18. SUPPLEMENTARY NOTES

19. KEY WORDS (Continue on reverse side if necessary and identify by block number)

SEP 0 9 1982

E

20. ABSTRACT (Continue on reverse side if necessary and identify by block number)

Stress depressions ~~(Δσ)~~ of hard elastic polypropylene, hard elastic high impact polystyrene, and Gore-Tex®, A nonelastic, porous, Teflon® material were measured when these polymers, under load, were subjected to changes in their environment from air to various nonswelling liquids. The stress depressions were studied as a function of liquid surface tension and viscosity and the strain imposed on the materials. Results indicate that these microfibrillated polymers contain a substantial surface energy

DD FORM 1 JAN 73 1473 EDITION OF 1 NOV 65 IS OBSOLETE
S/N 0102-014-6601

SECURITY CLASSIFICATION OF THIS PAGE (When Data Entered)

component in their stress which is independent of strain at high tension. This surface energy component is apparently inversely proportional to the average microfibril diameter. It is suggested that a maximum fibril diameter limit exists such that, above this limit, hard elastic behavior will not occur.

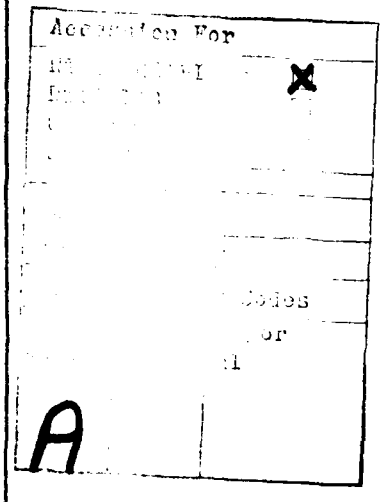

STRESS RELATED SURFACE TENSION EFFECTS IN HARD ELASTIC POLYMERS

Kim Walton, Abdelsamie Moet and Eric Baer
Case Western Reserve University
Department of Macromolecular Science
Cleveland, Ohio 44106

INTRODUCTION

Many investigators have invested a sizeable amount of effort in the study of specially processed polymers, known collectively as hard elastic, since their patenting in the mid 1960's [1]. These materials have an unusual combination of physical and mechanical properties. Figure 1 shows the loading cycle of hard elastic polypropylene, and is typical behavior for these materials. Some examples include: 1) high initial modulus, 2) large recoverability (up to 98%), 3) 'energetic' elasticity, and 4) high porosity. This field was thoroughly reviewed by Cannon, McKenna, and Statton in 1976 [2].

The first hard elastic polymers were made from crystalline lamellar materials, and were processed via melt spinning and stress crystallization, followed by annealing under tension. The common morphology of these polymers is shown for hard elastic polypropylene [3] in Figure 2a. The structure consists of rows of lamellae oriented perpendicularly to the direction of draw. Between these lamellae are microfibrils (ca. 100-500Å diameter) parallel to the draw direction and interspaced with voids.

Over the years, several different models were proposed in an attempt to relate the mechanical behavior to the morphology,

most of which involved a bending or shearing mechanism of the row-structured lamellae [4,5]. Hence, crystallinity was thought an essential criterion for hard elastic behavior. However, microscopic investigations by Miles, et. al. [6] of hard elastic polyethylene revealed little distortion of the lamellae. Further, calorimetric studies by Görtz and Müller [7] indicated both energetic and entropic elastic components, unaccounted for by the lamellae model.

Attention in more recent models has been given to the free surface energy change of the polymers with strain [6-9]. Furthermore, the focus has changed from the lamellae to the microfibrils.

An analogous microstructure can be produced in amorphous polymers by crazing them. Figure 2b shows the similarity of the craze structure to the crystalline morphology. We have reported that extensively crazed high-impact polystyrene (HIPS) exhibits hard elastic behavior, as the loading cycle illustrated in Figure 3 shows [10,11]. Hence, hard elastic behavior is associated with a bulk-microfibril composite structure and is independent of crystallinity. We believe that a substantial portion of the elastic restoring force is due to a surface energy mechanism associated with the fibrils.

Evidence for the above hypothesis is demonstrated by the unique behavior of the stress in extended hard elastic materials to "inert" liquids. The phenomenon was first reported by Miles, et. al. [6] with polyethylene and further studied by our group using HIPS [11]. Figure 4 shows the experimental procedure. The sample was stretched to a desired fixed elongation and the stress

was allowed to relax to a time independent level. While under fixed elongation, the sample was immersed in a non-swelling wetting liquid. Immediately, the stress dropped to a new level, remaining there until the liquid was removed; subsequently, the stress rose to a new level. Liquids with high surface tensions (non-wetting) induced no change in the stress, whereas low surface tension liquids (wetting) produced a substantial depression of the stress.

Recently, Brown and Kramer have reported a study of the rise in stress after changing the environment of crazed polystyrene specimens under load from methanol, water or their mixtures to air [12]. They derived an equation relating the change in the surface component of the stress to the surface tension and the craze fibril geometry.

In this study, we closely examine the stress depression phenomenon as a function of environmental surface tension, strain, and viscosity. These results are correlated with changes in the void content as the specimens are strained. Three systems are investigated: hard elastic HIPS, hard elastic polypropylene and Gore-Tex®, a non-elastic (see Figure 5) but fibrillated Teflon material (see micrograph in Figure 2c).

EXPERIMENTAL

Ordinary HIPS, supplied by the Dow Chemical Company, hard elastic polypropylene from Celanese Corporation, and Gore-Tex®, supplied by Gore and Associates, were the materials used in all experiments. The pellatized HIPS were compression molded into 10 mil thick sheets. Dumbbell-shaped specimens about 3mm wide with a 16mm gauge length were cut from these sheets. The samples were annealed in a vacuum oven at 86°C for 50 hours then cooled

at 10°C/hr to room temperature to relieve internal residual stresses. Specimens of hard elastic polypropylene and Gore-Tex® were cut from 1 mil films, as received, using the same sample goemetry. Hard elastic HIPS was produced by straining the specimens in an Instron machine at a rate of 3×10^{-2} min^{-1} to an elongation of 40%, followed by immediate unloading. Stress-strain and stress relaxation experiments in air and in liquids were performed using an Instron tensile testing machine. The materials were strained to the desired fixed elongation and the stress was allowed to relax for one hour. Samples were then immersed in liquid and the stress was allowed to stabilize for 30 minutes, after which the liquid was drained, resulting in a new stress level after a period of ten minutes.

Void volume estimates as a function of strain were obtained by stretching the preweighed porous samples to a fixed elongation and imbibing them with 5cSt silicone oil. Excess oil was carefully wiped from the surfaces. After unloading the tension from the samples, oil was forced out of the contracting material and absorbed by preweighed pieces of filter paper. The total mass of the oil imbibed in the strained specimens were then determined by weight difference.

RESULTS

The effect of surface tension of environmental liquids on the stress depression, $\Delta\sigma$, was studied by straining the materials to 25% and then following the immersion procedure described above using firstly, pure, non-swelling liquids and finally, water-ethanol mixtures. The weight fraction of ethanol in the mixtures was varied for different samples and the resultant stress

depression was measured as a function of the surface tension of the mixture [13]. Table 1 shows the effects of various pure liquids on the stress depression of the three materials. The liquids are listed with their surface tensions (γ) in descending order. Note that, generally, the stress depressions increase with decreasing environmental surface tension. Furthermore, the observed values for surface tension above the critical wetting energy of the polymers, γ_c, are very small or zero. However, the magnitude of the observed depressions differed substantially with the material under tension. Overall, Gore-Tex® exhibited stress changes about two orders of magnitude lower than HIPS and hard elastic polypropylene.

Figures 6a and 6b show the relationships between the surface tension of the water-ethanol mixtures and the stress depressions exhibited by hard elastic HIPS and hard elastic polypropylene, respectively. For hard elastic HIPS, pure ethanol (γ = 22.5 dynes/cm) induced a change of 31.3 kg/cm^2. A dramatic decrease in the stress drop was observed when the surface tension of the mixtures was increased from 22.5 to 25 dynes/cm. This was followed by a more gradual decrease in the depression with surface tension. The most interesting feature to note is the inflection at γ = 35-40 *dynes/cm*. This value corresponds closely to the critical surface energy of polystyrene reported elsewhere [14]. Beyond this transition there was little change in the stress depression as the surface tension increased. Note the change in slope at the inflection from 1.5 to 0.25 kg/cm

dynes with increasing surface tension. A similar relationship was exhibited by hard elastic polypropylene as shown in Figure 6b. There are important differences, however. The stress depression values are much larger than HIPS (112 kg/cm^2 in ethanol); furthermore, no changes in stress were observed above 40 dynes/cm, close to the critical wetting energy [5] of polypropylene. Water-ethanol mixtures were not used for Gore-Tex® since the surface tensions of the mixtures are too high. Thus, Figure 7 shows a stress depression-surface tension plot for Gore-Tex® using pure liquids. Note the small drop in stress overall; also observe that no depressions exist at surface tension values above 22 dynes/cm, a value close to σ_c for Teflon® [16].

The stress depression is believed to be very sensitive to the microfibril structure. Thus, this phenomenon was further investigated as a function of the polymer deformation and subsequent change in structure. Hard elastic samples were stretched to different fixed elongations and the observed changes in stress resulting from immersion in methanol were measured. These values were normalized with the corresponding initial equilibrium stress, σ_o. Figure 8 compares the effect of strain on the normalized stress depression, $\Delta\sigma/\sigma_o$. As shown for HIPS, the normalized stress drop increased linearly with strain up to 25%, remaining constant thereafter. On the other hand, normalized values for hard elastic polypropylene remained essentially constant for all elongations.

The stress depressions observed for hard elastic polypropylene and Gore-Tex® were completely reversible ($\sigma_f=\sigma_o$). Hard elastic HIPS,

however, exhibited a stress drop, $\Delta\sigma_r$ (Figure 4). As shown in Figure 9, the dependence of the residual stress change on strain was very similar to the $\Delta\sigma/\sigma_o$ relationship. Below 15% elongation, however, upon removal of the methanol environment, the stress rose to a level exceeding the initial equilibrium stress. This is shown as a negative residual stress depression. The pore characteristics of the hard elastic polymers were determined by two methods. First, the effect of liquid viscosity on the stress drop was studied. Next, the void volume changes with strain were examined. Figure 10 illustrates the effect of liquid viscosity on the stress drop. In this experiment, silicone oils of different viscosities were used. As can be seen, the overall shape of the stress curves changes from a rapid stress drop to a more gradual stress reduction as the viscosity was increased from 1 to 5000 cSt for subsequent samples.

Because of its low evaporation rate, silicone oil remains entrapped in the pores of these materials. This imbibing quality was utilized to obtain a rough estimate of the void volume fraction of hard elastic HIPS and polypropylene as a function of strain. These values are only estimates since the oil may not penetrate the smaller pores in the materials. The method, however, does offer a simple alternative to other techniques such as mercury porosimetry. As shown in Fig.11, the results for hard elastic polypropylene are, in fact, reasonably close to void volume fraction measurements determined by mercury penetration [4]. Note that a linear relationship exists between the void volume fraction and strain for hard elastic polypropylene; the slope of the line

is about one. On the other hand, void volume estimates for hard elastic HIPS are much lower overall (slope is about one-half). Furthermore, the crazed HIPS has a small initial void content at zero strain, whereas no measurable voids were detected for the unstrained hard elastic polypropylene film.

Despite an increase in void volume with strain, the stress depressions for hard elastic polypropylene are essentially strain independent. On the other hand, crazed HIPS showed significant elongation dependencies in its stress change. Apparently, subtle differences in the deformations of these materials are occurring.

DISCUSSION

The precise function of microfibrils in hard elastic polymers is not well understood. Their importance in various models of crystalline polymers has ranged from mere tie points [4,5] to the fundamental element [9]. The recent disclosure of hard elastic behavior in crazed HIPS [11] clearly revealed the connection between microfibrillar superstructure and hard elastic behavior, since no lamellae exists in this material. Polymers with a fibrillar structure are not necessarily hard elastic, however. Gore-Tex® has an extensive fibrillar domain as shown in Figure 2c. Its loading cycle (Figure 5), however, clearly reveals an inelastic material. Hence, the necessary criterion of microfibrillar structure for a hard elastic polymer must be established.

Microscopic investigations of hard elastic polymers indicated that extensive void and fibril formation occurs with strain [2,4,6]. Further studies with mercury porosimetry [17] and BET gas absorption [18] revealed a large internal surface area and a pore size hierarchy for deformed hard elastic polymers. Our

own experiments show significant void formation during extension. There are notable differences between hard elastic polypropylene and HIPS, however. As shown in Figure 11, the void volume is much more sensitive to strain for polypropylene than HIPS. Furthermore, the virgin polypropylene hard elastic film has very little void content, whereas crazed HIPS contains a significant initial void volume. These differences are primarily due to variations in processing for the two polymers.

Gas flow experiments [3] and our studies with different liquid viscosities (Figure 10) reveal that the voids are interconnecting and that fluid flow in these materials occurs by mass transport. The flow rate is greatly reduced in high viscosity fluids. One can conclude, therefore, that these materials exhibit mechanical behavior greatly influenced by load bearing microfibrils, open to the environment.

The stress sensitivity of hard elastic polymers to changes in environmental surface tension has been well documented [6,10,11]. Because of their exposure to the environment, the surface contribution to the stress is primarily due to the microfibrils. Brown and Kramer [12], using a cylinder as a model for craze fibrils related the change in the surface component of the stress in crazed polystyrene to the change in surface tension as shown below:

$$\Delta\sigma = \frac{2\,\Delta\gamma\,v_f}{\bar{D}} \qquad (1)$$

where v_f is the volume fraction of the craze fibrils, $\Delta\gamma = \gamma_{\text{polymer/air}} - \gamma_{\text{polymer/liquid}}$, and $\bar{D}$ is the average craze fibril diameter. The above equation predicts that the stress

depression is simply a function of the surface tension and fibril geometry of any polymer. Thus, Equation 1 should be applicable to all microfibrillated polymers.

A linear relationship between stress depression and the change in surface tension is predicted by this model. Figures 6a, 6b and 7 indicate that the stress depression - surface tension relationship can be reasonably approximated as linear for surface tension values below γ_c. Note that the surface tensions shown on the abscissa are liquid, rather than interfacial surface tensions. Nevertheless, these plots clearly reveal a monotonic relationship between $\Delta\sigma$ and $\Delta\gamma$.

Using interfacial surface tension values from the literature [12,14-16] for the environmental liquids chosen for the study, stress depression values can be calculated from Equation 1. The interfacial tension may also be estimated using Fowke's method [19]. The surface energy of the polymer and liquid are separated into dispersion and hydrogen bonding components, γ^d and γ^h. The relationship is given by

$$\gamma_{12} = [(\gamma_1^d)^{\frac{1}{2}} - (\gamma_2^d)^{\frac{1}{2}}] + [(\gamma_1^h)^{\frac{1}{2}} - (\gamma_2^h)^{\frac{1}{2}}]^2 \qquad (2)$$

where 1 corresponds to the liquid component and 2 corresponds to the polymer.

Table II shows stress depressions calculated from Equation 1 for the three polymers using exprimentally determined [12,14-16] and estimated [20] interfacial surface tension values for selected liquids. Calculated and experimental values are compared.

As predicted by Equation 1, the stress depression values

for Gore-Tex® are substantially lower since its average fibril diameter (~0.3 μm) is about two orders of magnitude larger than those of hard elastic HIPS and polypropylene. This low sensitivity to changes in surface tension implies that the surface component of the stress in Gore-Tex® is small.

Unfortunately, calculated and experimental stress depression values for hard elastic polypropylene are substantially different. Unless the fibril volume is much larger or the fibril diameter much smaller than previously reported [4-9], there is no suitable explanation for the discrepancies between the calculated and experimental values using this model.

Equation 1 further predicts that the stress depression is independent of strain. As seen in Figure 8, hard elastic polypropylene obeys this relationship (the raw stress depression values were also approximately constant). For hard elastic HIPS under high tension the stress depressions are independent of strain. Below about 25% elongation, however, the stress depressions decrease with strain. The effect may be due to a larger fibril diameter at low strains, or an increase in the volume fraction of the fibril phase with elongation. Again, the differences in process history contribute greatly to the differences in strain response.

Summarizing the comparisons between calculated values from Equation 1 and experimental results, we observe that:

1) Equation 1 correctly predicts a linear relationship between stress depression and liquid surface tension, at least for surface tension values below the critical wetting point.

2) As indicated by Equation 1, the stress depression is dependent on the diameter of the microfibrils under stress.

3) This surface phenomenon is independent of strain for hard elastic polypropylene for all elongations and for hard elastic HIPS above 25% strain.

4) The values of stress depression predicted by Equation 1 for hard elastic polypropylene, are, however, far lower than experimentally determined.

Therefore, although the cylindrical model works well as an approximation of the stress depression-surface tension phenomenon, the relationship is undoubtably more complicated than the geometric description given in Equation 1.

Another method of describing the stress sensitivity of these polymers to changes in surface tension is a phenomenological approach. Chudnovsky et al. [21] recently developed a theory of crazing in amorphous polymers. In this paper they postulated that a craze may be treated as a separate phase from the bulk. Evidence from previous work indicates that this postulate may be generalized for all microfibrillated polymers. Brown and Kramer [12] observed from micrographic evidence in other work [22] that the craze fibrils have a much greater compliance than the bulk glass. Takayanagi et al. [23] developed a two phase mechanical model for fibrillated crystalline polymers. The phases consisted of a crystalline and amorphous region and taunt tie (microfibril) molecules.

If we construct a parallel model of fibril and bulk phases (Figure 12), the total stress is the sum of the contributions of these two regions. Thus,

$$\sigma_{Total} = \sigma_{Bulk} + \sigma_{Fibrils} \qquad (3)$$

The stress components can be related to their respective moduli and the concentrations of either phase. In addition to its intrinsic material property, the fibril modulus has a surface tension component. For these phases in parallel,

$$\sigma = [(1-c)E_b + cE_f(1 + f(\gamma)]\varepsilon \qquad (4)$$

where:

E_b, E_f = modulus of bulk and craze fibrils, respectively

c = fractional fibril concentration

γ = interfacial surface tension

Hence, we attempt to relate the surface tension component to an intrinsic property, i.e., modulus of the polymer. Because of our limited knowledge of the interaction between the microfibrils and the liquid environment, the function $f(\gamma)$ cannot be explicitly derived. However, the differential form of $f(\gamma)$ can be estimated by imposing the restriction that ε is constant and that the material is in a stress relaxation mode. The change in the stress depression with respect to surface tension has been observed to be linear. Hence:

$$\Delta\sigma \simeq K\Delta\gamma \qquad (5)$$

where $\Delta\gamma = \gamma_{\text{polymer/air}} - \gamma_{\text{polymer/liquid}}$. Differentiating (4) with respect to γ we obtain:

$$\frac{\partial\sigma}{\partial\gamma}\, d\gamma = \left[\frac{\partial c}{\partial\gamma}(E_f - E_b) + E_f\, f(\gamma)\frac{\partial c}{\partial\gamma} + cE_f\frac{\partial f(\gamma)}{\partial\gamma}\right]\varepsilon\, d\gamma \qquad (6)$$

but from (5): $$\frac{\partial \sigma}{\partial \gamma} \simeq \frac{\Delta c}{\Delta \gamma} \simeq K$$

Therefore (4) rearranges to

$$K \simeq \left[\frac{\partial c}{\partial \gamma} (E_f - E_b) + E_f f(\gamma) \frac{dc}{\partial \gamma} + cE_f \frac{\partial f(\gamma)}{\partial \gamma}\right] \varepsilon$$

Surface tension changes are not thought to induce changes in the microfibril concentration. Thus (6) reduces to

$$K \simeq cE_f \frac{df(\gamma)}{d\gamma} \varepsilon \qquad (7)$$

K can be readily calculated using the stress depression values obtained experimentally and the literature values for the interfacial surface tensions of the polymers with various liquids [12,14-16,20]. Hence we obtain K values of 0.667 cm^{-1}, 2.78 cm^{-1}, and 4.92 x 10^{-2} cm^{-1} for HIPS, polypropylene, and Gore-Tex®, respectively. The fibril modulus of the polymers can be estimated using a method described by Coran and Petal [24]. The values obtained are 1.3 x 10^4 kg/cm^2, 1.8 x 10^4 kg/cm^2 and 1.1 x 10^3 kg/cm^2 for HIPS, hard elastic polypropylene and Gore-Tex®, respectively.

From the literature [4,12], fibril concentrations of 0.2 and 0.5 are assumed for HIPS and hard elastic polypropylene. Our own microscopic investigations of Gore-Tex® revealed a fibril concentration of 0.5. Using these values, estimates of $\frac{df(\gamma)}{d\gamma}$ were 1.03 x 10^{-3} cm/dyne , 1.24 x 10^{-3} cm/dyne, and 3.58 x 10^{-4} cm/dyne for HIPS, hard elastic polypropylene and Gore-Tex®. Further investigations of the exact nature of the microfibril - liquid interaction are needed to derive an explicit function.

We have stated previously that a microfibrillar structure is a necessary requirement for hard elastic behavior. Note, however, that this structure is not a sufficient condition. Gore-Tex® is clearly non-elastic. We have further noted that the surface component of the stress in this polymer is apparently rather low, resulting in its small sensitivity to changes in environmental surface tension. An apparent reason for this low reactivity is its relatively large average fibril diameter.

One may conclude, therefore that the microfibrils in the structure must have a sufficiently low diameter in order to induce hard elastic behavior. There are two justifications for this conclusions. Firstly, we have observed that hard elastic polymers contain a large surface tension component in their retractive stress, an observation supported by Miles et. al. [6] and postulated by others [7-9]. The surface component of the stress in Gore-Tex®, as shown by our experimental evidence and predicted by Equation 1, is simply too small to induce a suitable retractive force.

Secondly, fibrils with a relatively large diameter are more likely to exhibit bulk-like behavior, or, in other words, be subjected to a triaxial stress field. As shown in Figure 13, large fibril units under a stress below the yield (A&B) contain a triaxial stress state and are subject to drawing or necking. At stress levels sufficiently higher than the yield stress, narrow fibrils are under uniaxial stress (C). Thus, because of their very small diameter, the microfibrils in hard elastic polymers are subjected to, primarily, uniaxial stress. Craze

fibrils in particular do not neck but grow by drawing material from the bulk [22].

Hence, a maximum fibril diameter limit exists where "microfibrillar" behavior occurs. By microfibrillar behavior, we refer to their high elasticity [12] and large surface energy component in their stress. It is our belief that hard elastic behavior is a bulk manifestation of the mechanical properties of microfibrils. Thus, above a certain average fibril diameter level, hard elastic behavior will not occur. This bulk-to-microfibril transition diameter is, no doubt, characteristic of the particular polymer. Determination of this critical fibril diameter in the future will lead to greater understanding of the structural criterion for hard elastic behavior.

The question of swelling or solvation is a difficult one since surface tension and solubility parameter are closely related [12]. Note, however, that, particularly for hard elastic polypropylene and Gore-Tex®, the stress depression phenomenon is both rapid and reversible. The residual stress depression in HIPS, however (Figure 9), appears to be a measure of permanent damage to the material. For liquids with solubility parameters close to polystyrene, residual depression values were high. The large degree of crystallinity in isotactic polypropylene and Teflon® probably prevented similar occurrences for hard elastic polypropylene and Gore-Tex®.

CONCLUSIONS

Hard elastic polymers consist of numerous interconnecting pores whose void volume is highly dependent on the processing

history and strain imposed on the materials. Mass transport of fluids into these pores is greatly affected by the viscosity of the environmental liquid, decreasing with increasing viscosity.

Hard elastic behavior is a manifestation of a bulk-microfibril superstructure. A substantial surface energy component of the stress exists in these materials, independent of strain at high tension. As a result, significant changes in the equilibrium stress occurs when these polymers, under load, are subjected to changes in environmental surface tension. An apparent requirement for this surface tension component is load bearing microfibrils with sufficiently small radii. Evidently, a maximum average fibril diameter exists whereby hard elastic behavior may occur in polymers with these structures.

Although the surface energy component of the stress is highly dependent on the fibril structure, the relationship between stress and structure is more complex than a simple geometric function. A phenomenological approach may give greater insight into this relationship. However, further knowledge of microfibrillar behavior in general is necessary to derive an explicit function.

ACKNOWLEDGEMENTS

We greatly appreciate the generous financial support of the Office of Naval Research through grant number 00014-75-C-0795 and the National Science Foundation through grant number DMR77-24952. We are also indebted to C. Brown of Celanese Corporation who supplied hard elastic polypropylene film, J. Hoover of W. L. Gore and Associates, Inc., for donating samples of Gore-Tex® through Professor J. Anderson, and

Professor A. Chudnovsky for many useful discussions. The contribution of L. Kim to experimental work in hard elastic polypropylene is also gratefully acknowledged.

REFERENCES

1. Celanese Corp. of America, B.P. 650 890 (January, 1965), Canadian Ltd., B.P. 962 231 (July 1, 1964), etc.

2. S. L. Cannon, G. P. McKenny and M. O. Statton, Macromol. Rev., 1, 209 (1976).

3. Celanese Plastics Company, Technical Bulletin, March 1977.

4. B. S. Sprague, J. Macromol. Sci., -Phys., B8(1-2), 157 (1973).

5. H. D. Noether and W. Whitney, Kolloid Z. F. Polymere, 251, 991 (1972).

6. M. J. Miles, J. Petermann and H. Gleifer, J. Macromol. Sci. -Phys., B12(4); 549 (1976).

7. D. Goritz and F. H. Muller, Coll. Polym. Sci., 253, 844 (1975).

8. R. P. Wool, J. Poly. Sci., Polym. Phys., Ed. 14, 603 (1976).

9. R. Hosemann and H. Cackovic, Coll. Polym. Sci., 259, 15 (1981).

10. M. J. Miles and E. Baer, J. Mater. Sci., 14, 1254 (1979).

11. A. Moet, I. Palley and E. Baer, J. Appl. Phys., 51 5175 (1980).

12. H. R. Brown and E. J. Kramer, Polymer, 22, 687 (1981).

13. A. W. Adamson, Physical Chemistry of Surfaces, Interscience, N. Y., p. 75 (1967).

14. D. W. Van Kvevelen, Properties of Polymers, Elsevier, Amsterdam.

15. A. H. Ellison and W. A. Zisman, J. Phys. Chem., 58 260 (1954).

16. H. W. Fox and W. A. Zismann, J. Colloid Sci., 5, 514 (1950).

17. R. G. Quynn et al., J. Macromol. Sci. -Phys., B4(4), 953 (1970).

18. Ibid, B5(4),721 (1971).

19. F. M. Fowkes, Ind. Eng. Chem., 56, 40 (1964).

20. O. K. Owens and R. C. Wendt, J. Appl. Polym. Sci. 13, 1741 (1969).

21. A. Chudnovsky, I. Palley and E. Baer, J. Mater. Sci., 16 35 (1981).

22. H. R. Brown and I. M. Ward, Polymer 14 469 (1973).

23. M. Takayanagi, K. Imada and T. Kajiyama, J. Polym. Sci. C, 15, 263 (1966).

24. A. Y. Coran and R. Patel, J. Appl. Polym. Sci., 20, 3005 (1976).

FIGURE LEGENDS

Figure 1 Typical hard elastic behavior demonstrated by the loading cycle of hard elastic polypropylene. Note hysteresis loop.

Figure 2 Electron micrograph of three different fibrillated polymers a) hard elastic polypropylene b) crazed polystyrene c) Gore-Tex®, a Teflon material.

Figure 3 Loading cycle of 40% crazed HIPS, clearly indicating hard elastic behavior.

Figure 4 Experimental procedure for measuring the stress depression. The difference between the initial equilibrium stress and the new stress level induced by liquids is called $\Delta\sigma_l$. The difference between the final stress after liquid removal and the initial stress is called $\Delta\sigma_r$.

Figure 5 Loading cycle of Gore-Tex® a highly inelastic material.

Figure 6 The effect of environmental surface tension on the stress depression in a) hard elastic HIPS and b) hard elastic polypropylene (HEPP) using water ethanol mixtures.

Figure 7 The $\Delta\sigma$-γ relationship of Goretex determined with pure liquids.

Figure 8 The effect of strain on the normalized stress depression of HIPS and HEPP.

Figure 9 The normalized residual stress depression measured for crazed HIPS as a function of (fixed) strain.

Figure 10 The effect of viscosity on the stress drop in hard elastic HIPS.

Figure 11 Void volume fraction of hard elastic HIPS and polypropylene as a function of strain.

Figure 12 Diagram of fibrillar and bulk phase in hard elastic polymers.

Figure 13 Schematic representation of the stress field in large (B) and small (C) fibrils.

TABLE I. DEPRESSION OF STRESS DUE TO IMMERSION IN LIQUID ENVIRONMENTS

Liquid	Surface Tension (dynes/cm)	Goretex	Stress Depression (kg/cm^2) HIPS*	HE Polypropylene
Water	72.0	0	0	0
Formamide	58.2	0	4.5	0
Ethylene Glycol	45.2	0	8.7	0
Methanol	24.5	0	25.9	90.4
Ethanol	22.5	0.31	31.3	112.2
Silicone Oil (8.3 cP)	19.7	0.63	21.4	227.4
n-Hexane	18.4	0.91	53.9	230.6
Freon (E-3)	14.2	2.23	13.5	199.5
* data taken from [11]				
Critical Surface Tension, γ_c (dynes/cm)	--	18.5[a]	42[b]	35[c]

a - [14]

b - [15]

c - [16]

TABLE II. COMPARISON OF CALCULATED AND EXPERIMENTALLY DETERMINED LIQUID INDUCED STRESS DEPRESSIONS

Hard Elastic HIPS (γ_c = 42 dynes/cm)

Liquid	γ_l(dynes/cm)	γ_{12}	$\Delta\gamma=\gamma_{p/air}-\gamma_{p/liquid}$	$\Delta\sigma_{cal}$ (kg/cm^2)	$\Delta\sigma_{exp}$
Water	72.0	43.5[a]	-1.5	-1.5	0
Methanol	25.0	3.0[a]	39	26.0	25.9
Hexane	18.4	5.2[a]	36.9	24.5	53.9
Freon E-3	14.2	27.7[a]	14.3	9.5	13.5

Hard Elastic Polypropylene (γ_c = 35 dynes/cm)

Liquid	γ_l(dynes/cm)	γ_{12}	$\Delta\gamma=\gamma_{p/air}-\gamma_{p/liquid}$	$\Delta\sigma_{cal}$ (kg/cm^2)	$\Delta\sigma_{exp}$
Water	72.0	52.5[a]	-17.5	-8.8	0
Methanol	25.0	2.5[b]	32.5	16.3	90.4
Hexane	18.4	2.64[b]	32.4	16.2	230.6
Freon E-3	14.2	4.6[b]	30.4	15.2	199.5

Gore-Tex® (γ_c = 18.5 dynes/cm)

Liquid	γ_l(dynes/cm)	γ_{12}	$\Delta\gamma=\gamma_{p/air}-\gamma_{p/liquid}$	$\Delta\sigma_{cal}$ (kg/cm^2)	$\Delta\sigma_{exp}$
Water	72.0	41[a]	-22.5	-0.75	0
Methanol	25.0	0.237[a]	18.3	0.60	0
Hexane	18.4	0.500[a]	18.0	0.60	0.9
Freon E-3	14.2	4.3[a]	14.2	0.58	2.23

a - Calculated from data of Owens and Wendt [20]

b. - Determined by assuming the hydrogen bonding component in polypropylene was zero [19]

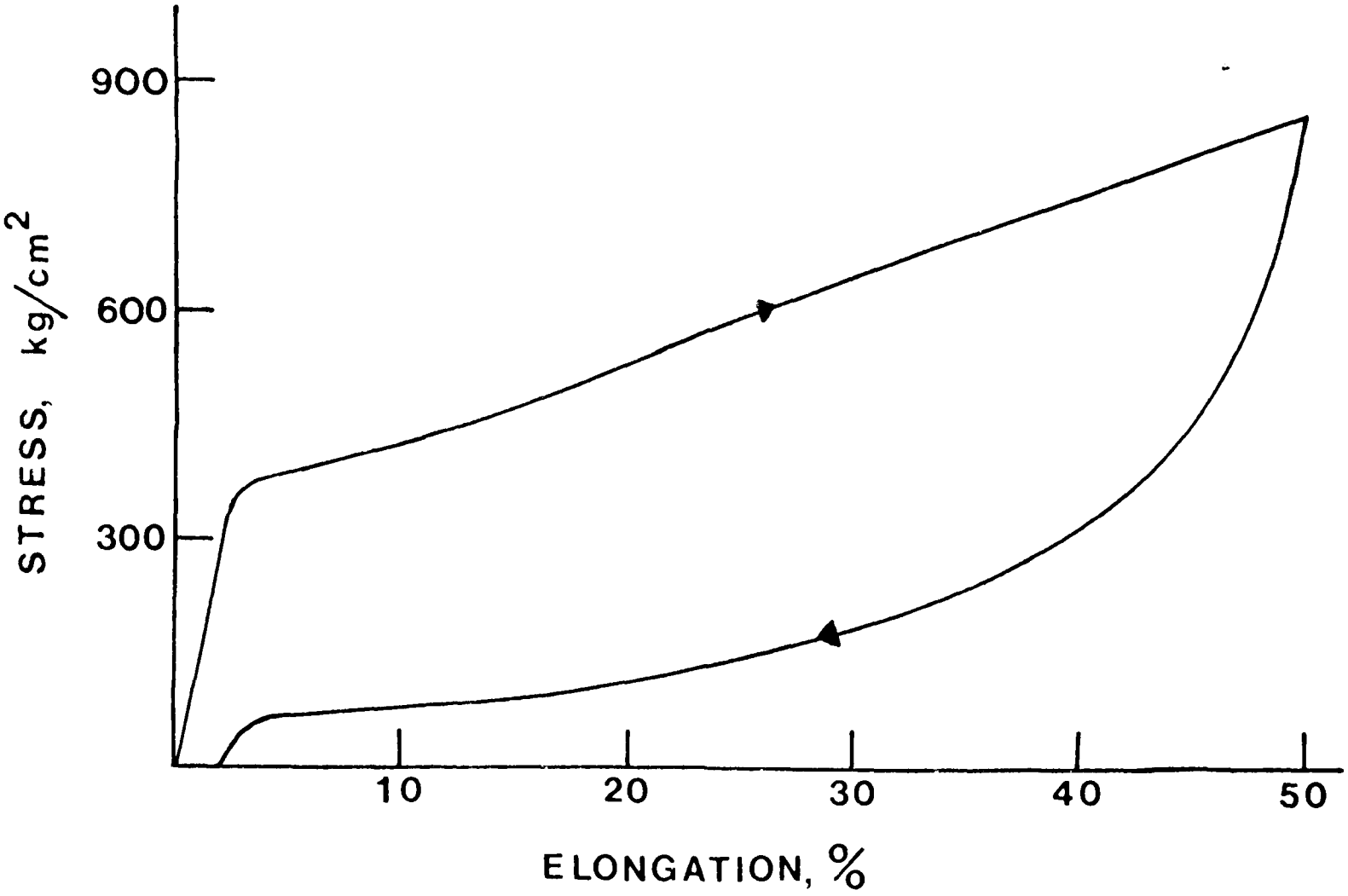

FIGURE 1

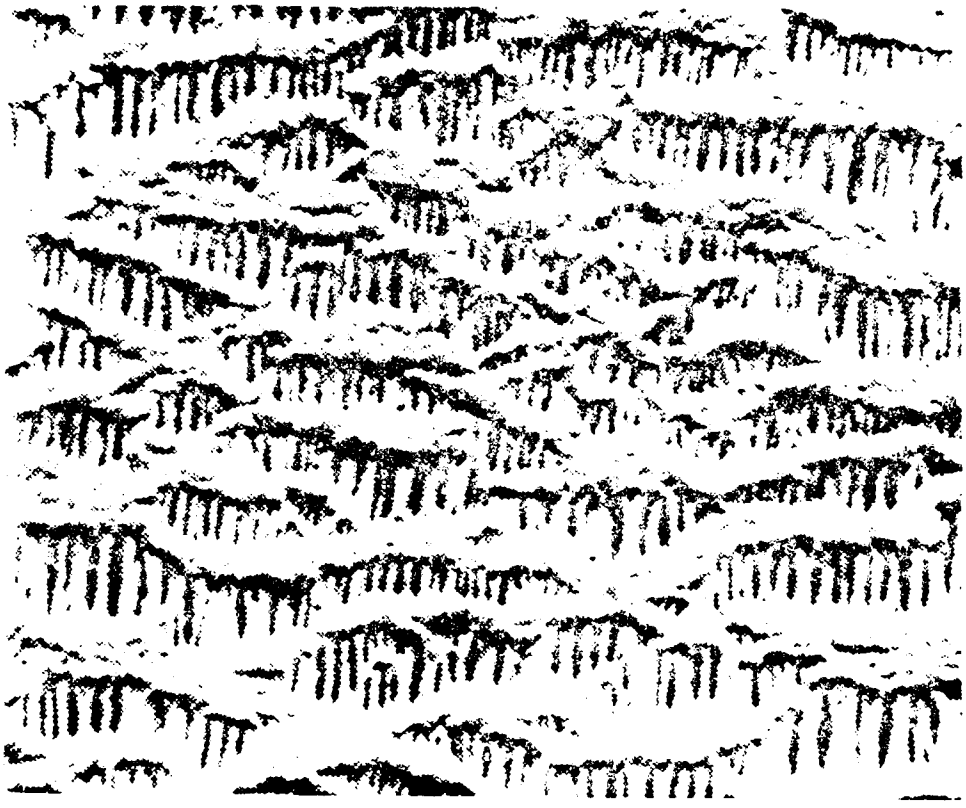

FIGURE 2a

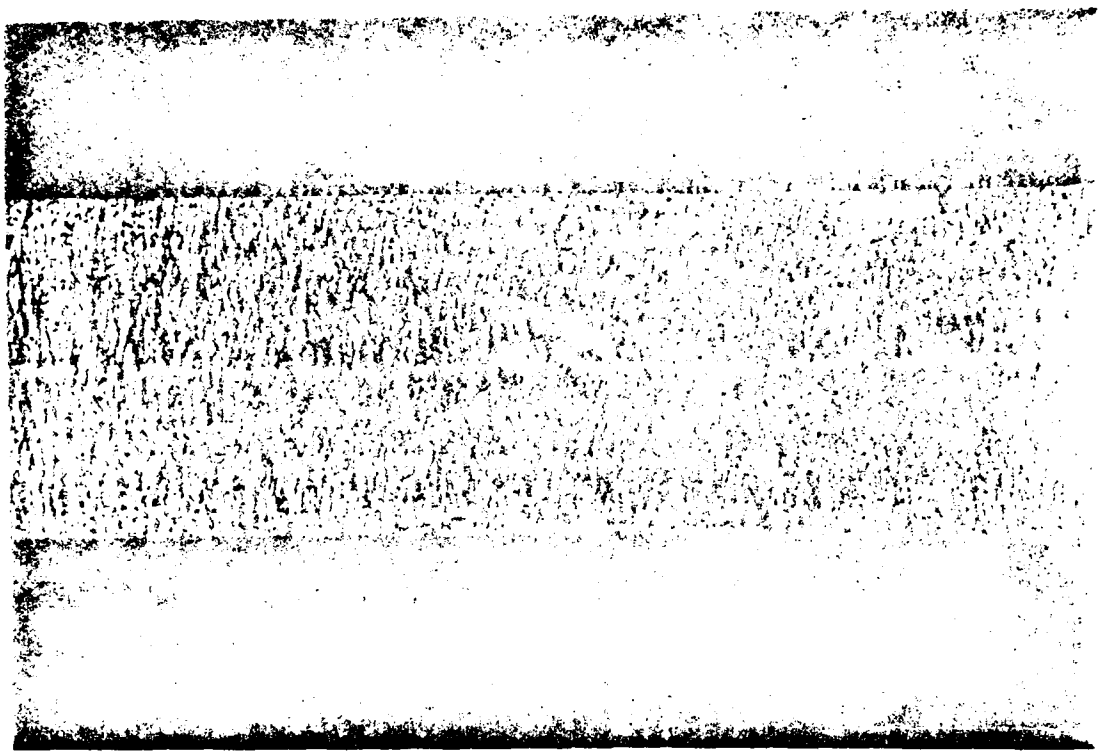

b)

1 μm

FIGURE 2b

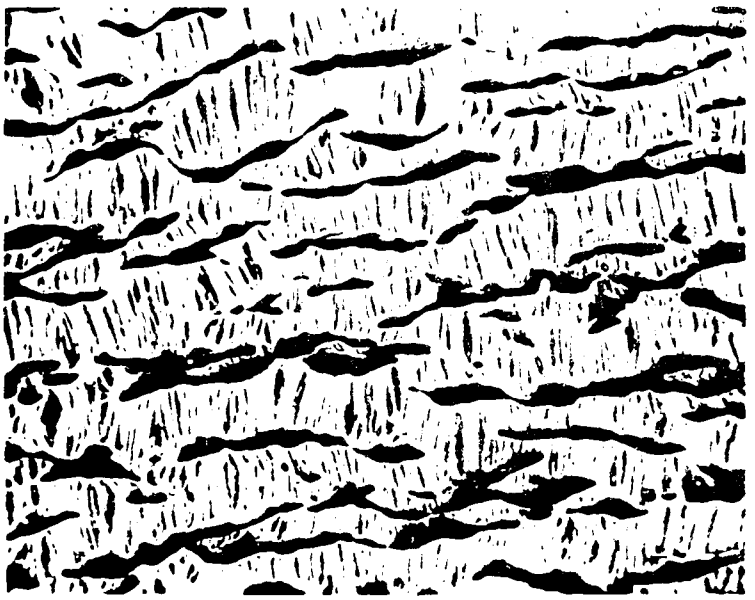

c)

40 µm

FIGURE 2c

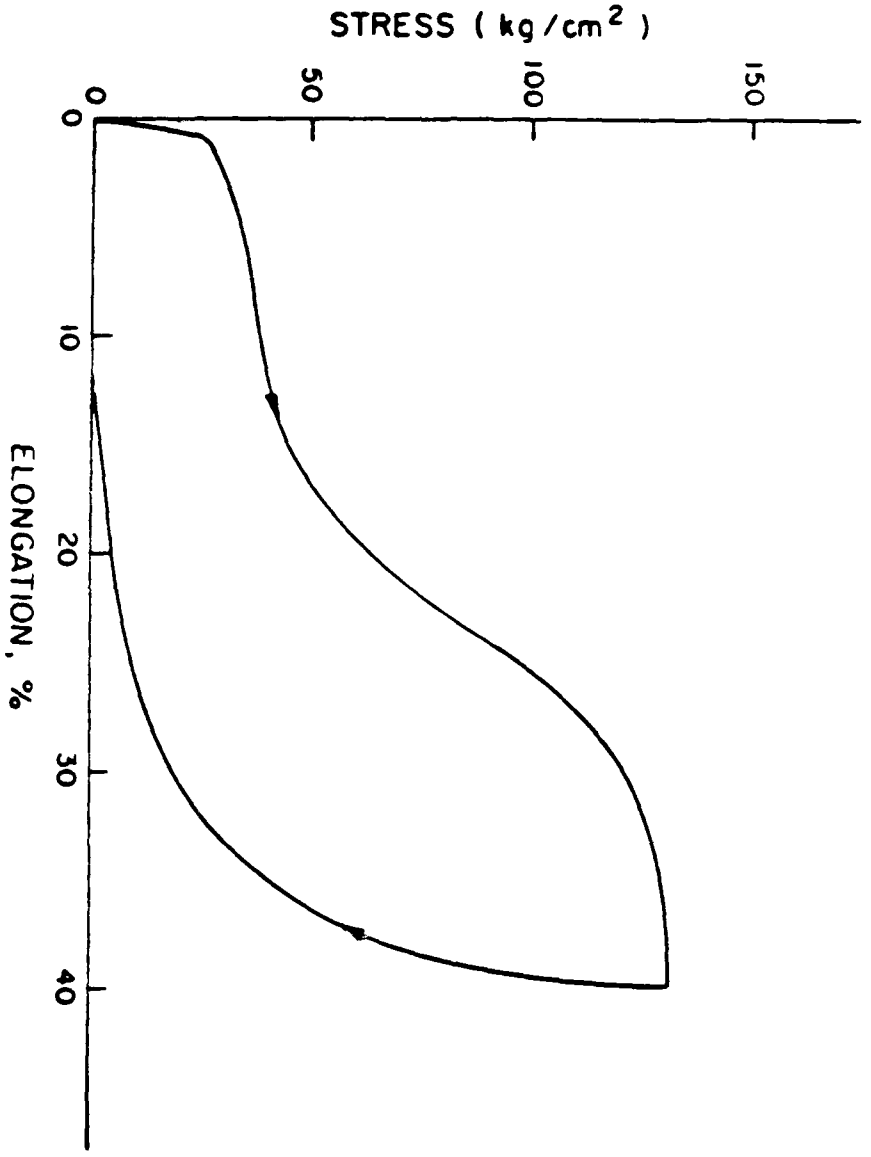

FIGURE 3

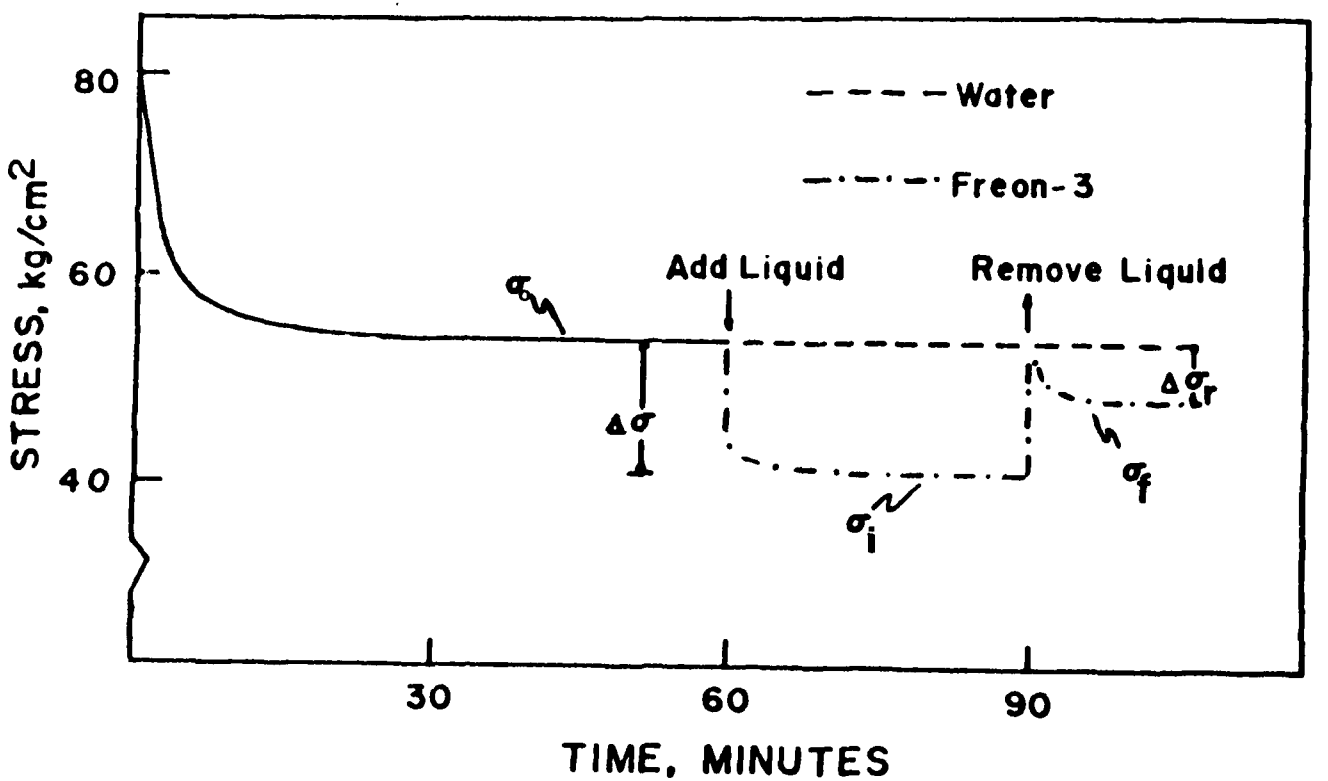
80
60
40
STRESS, kg/cm²
Water
Freon-3
Add Liquid
Remove Liquid
σ_o
$\Delta\sigma$
σ_i
σ_f
$\Delta\sigma_{cr}$
30
60
90
TIME, MINUTES

FIGURE 4

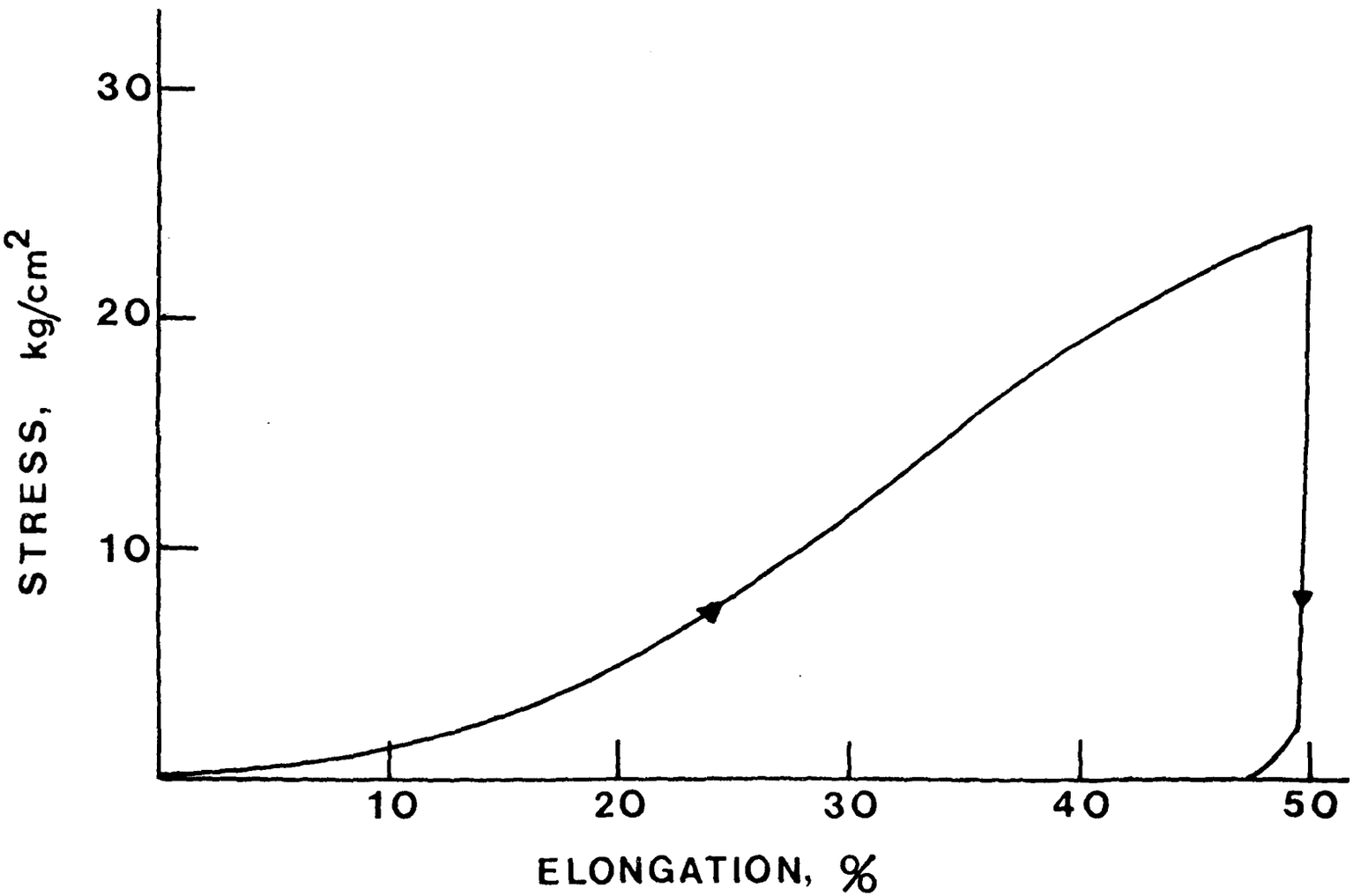

FIGURE 5

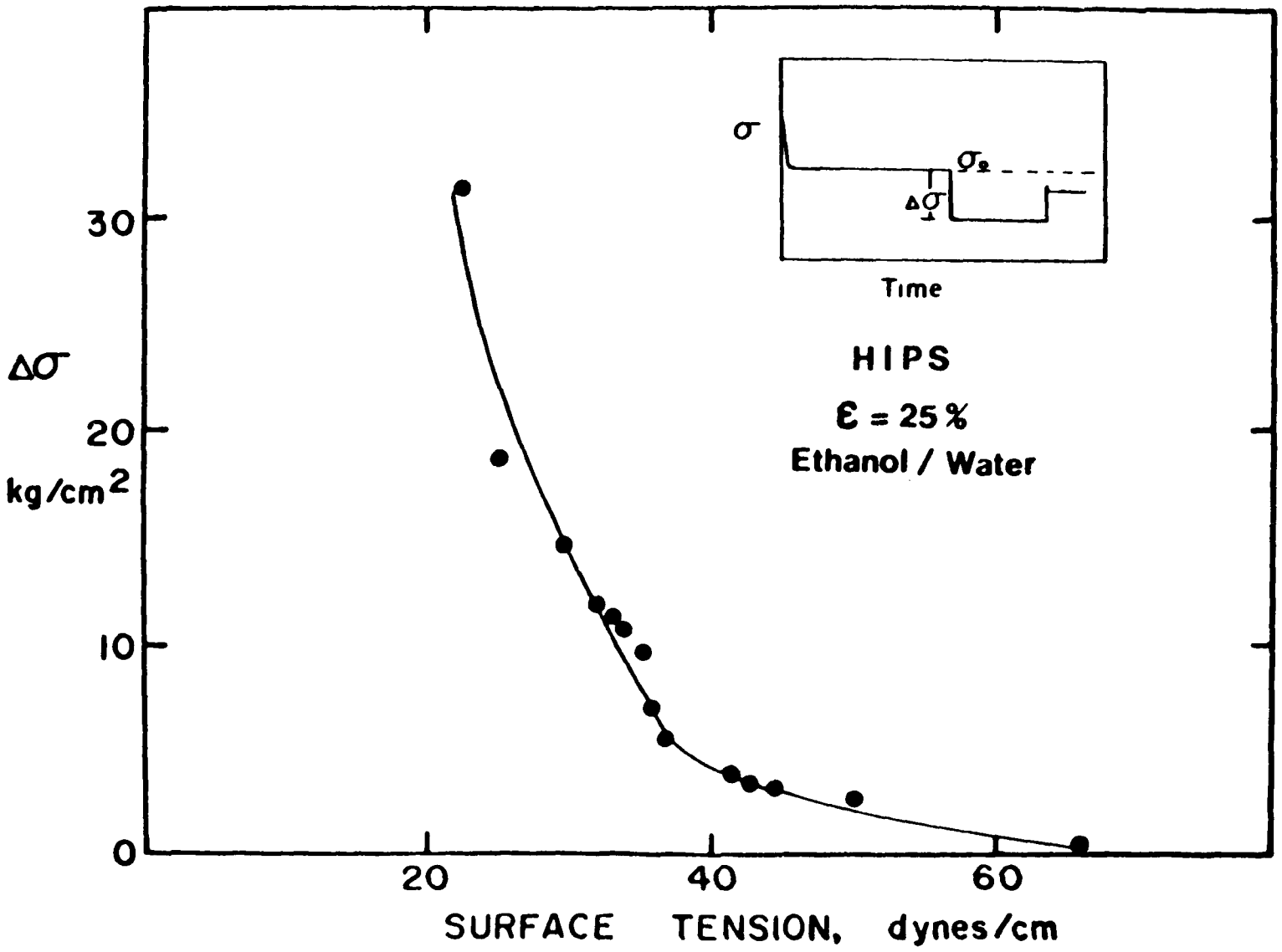
σ
σ₂
Δσ
Time
HIPS
ε = 25 %
Ethanol / Water
Δσ
kg/cm²
30
20
10
0
20
40
60
SURFACE TENSION, dynes/cm

FIGURE 6a

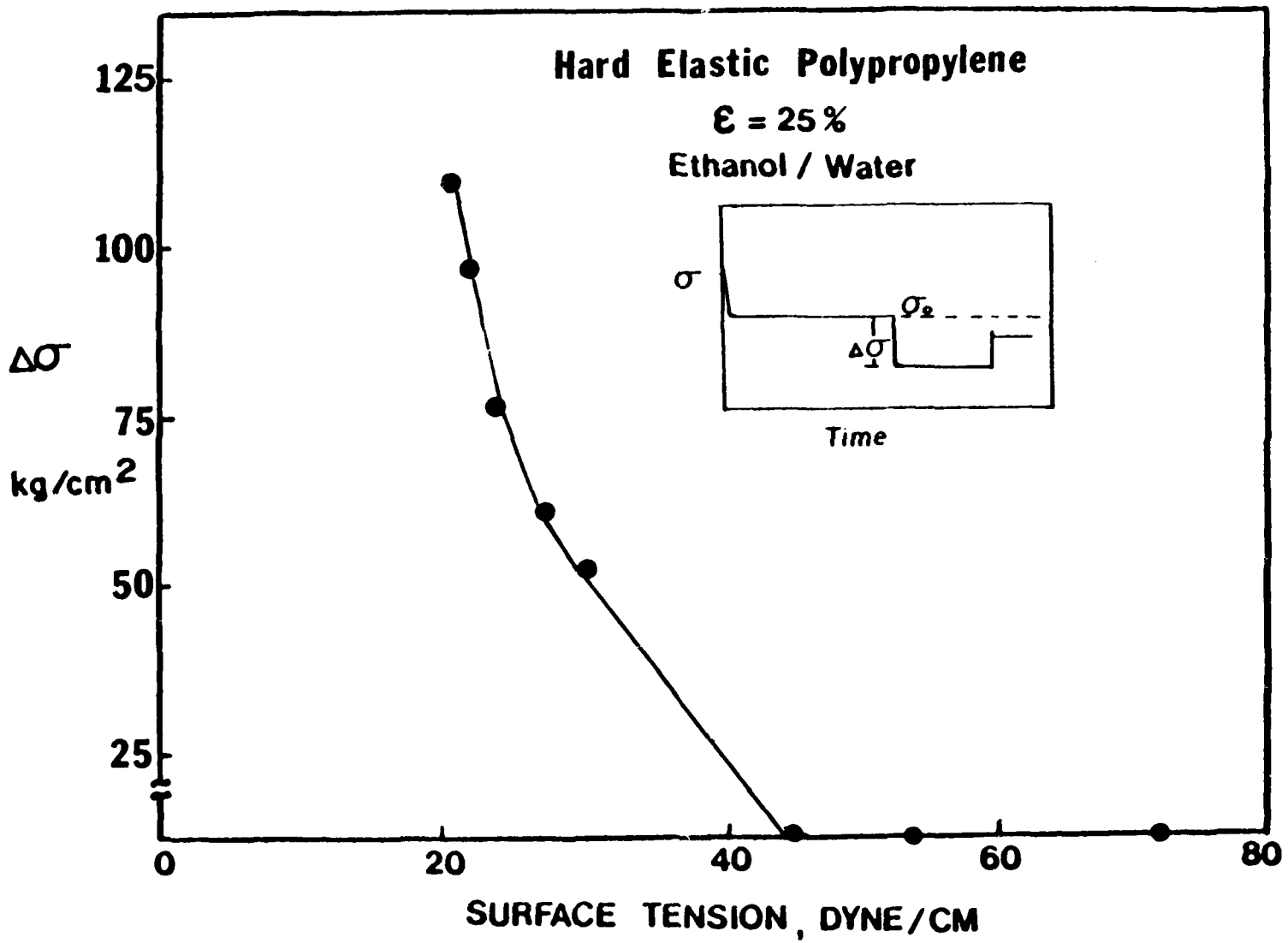
Hard Elastic Polypropylene
ε = 25 %
Ethanol / Water
σ
σ₂
Δσ
Time
125
100
75
50
25
Δσ
kg/cm²
0
20
40
60
80
SURFACE TENSION, DYNE/CM

FIGURE 6b

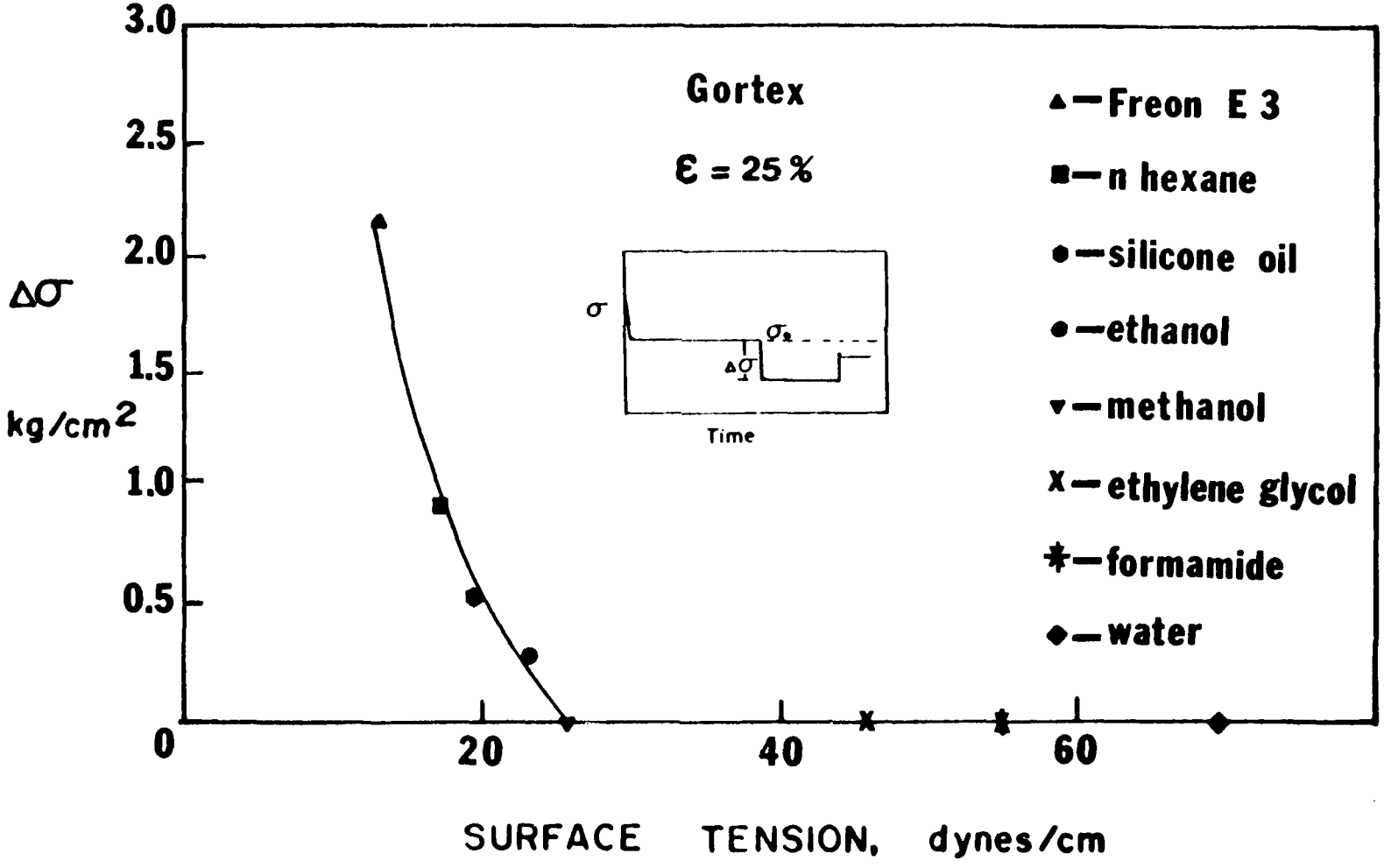
3.0
2.5
2.0
1.5
1.0
0.5
0
ΔσT
kg/cm2
Gortex
ε = 25 %
σ
σ₂
Δσ
Time
▲—Freon E 3
■—n hexane
●—silicone oil
●—ethanol
▼—methanol
x—ethylene glycol
✱—formamide
◆—water
20
40
60
SURFACE TENSION, dynes/cm

FIGURE 7

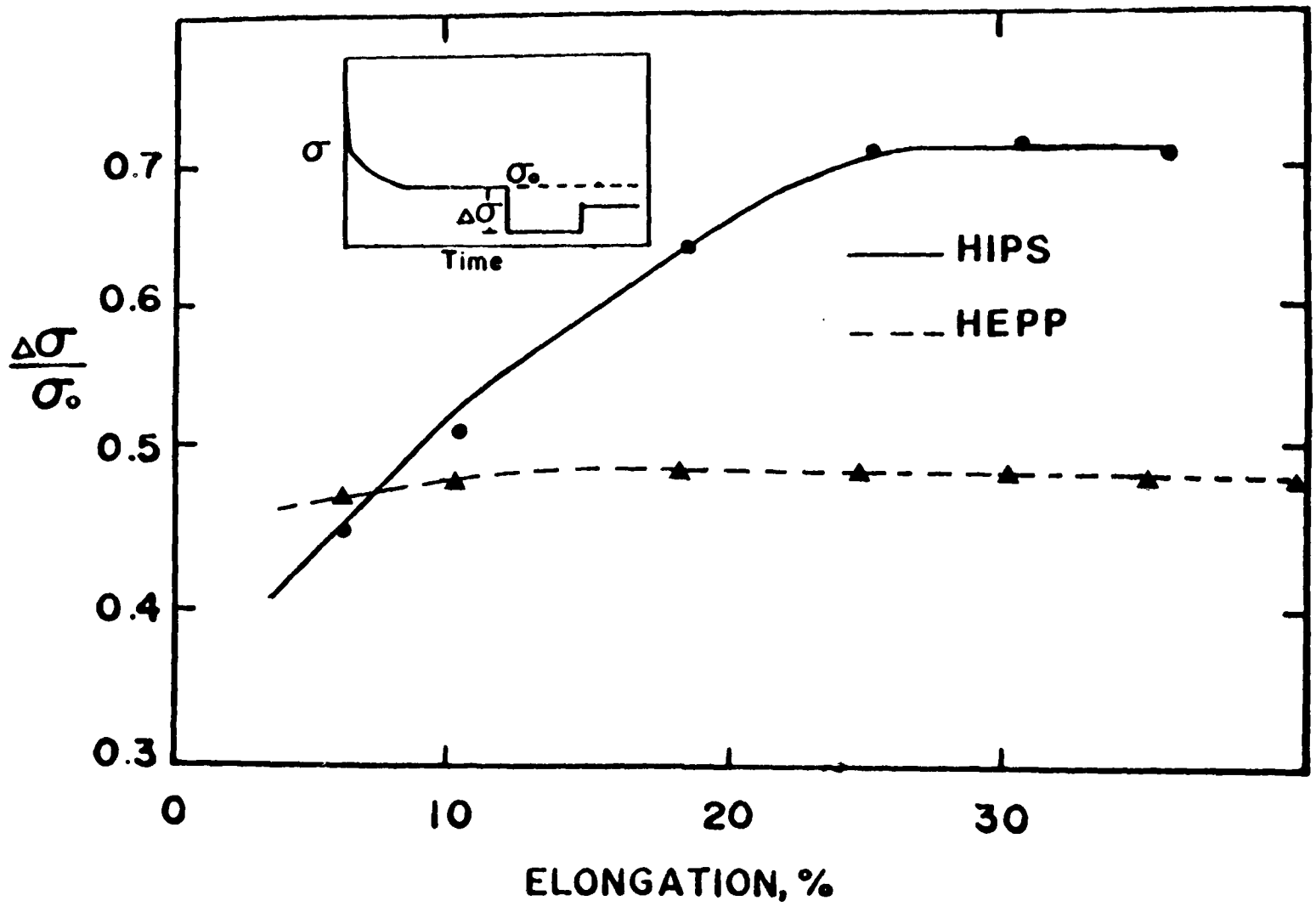

FIGURE 8

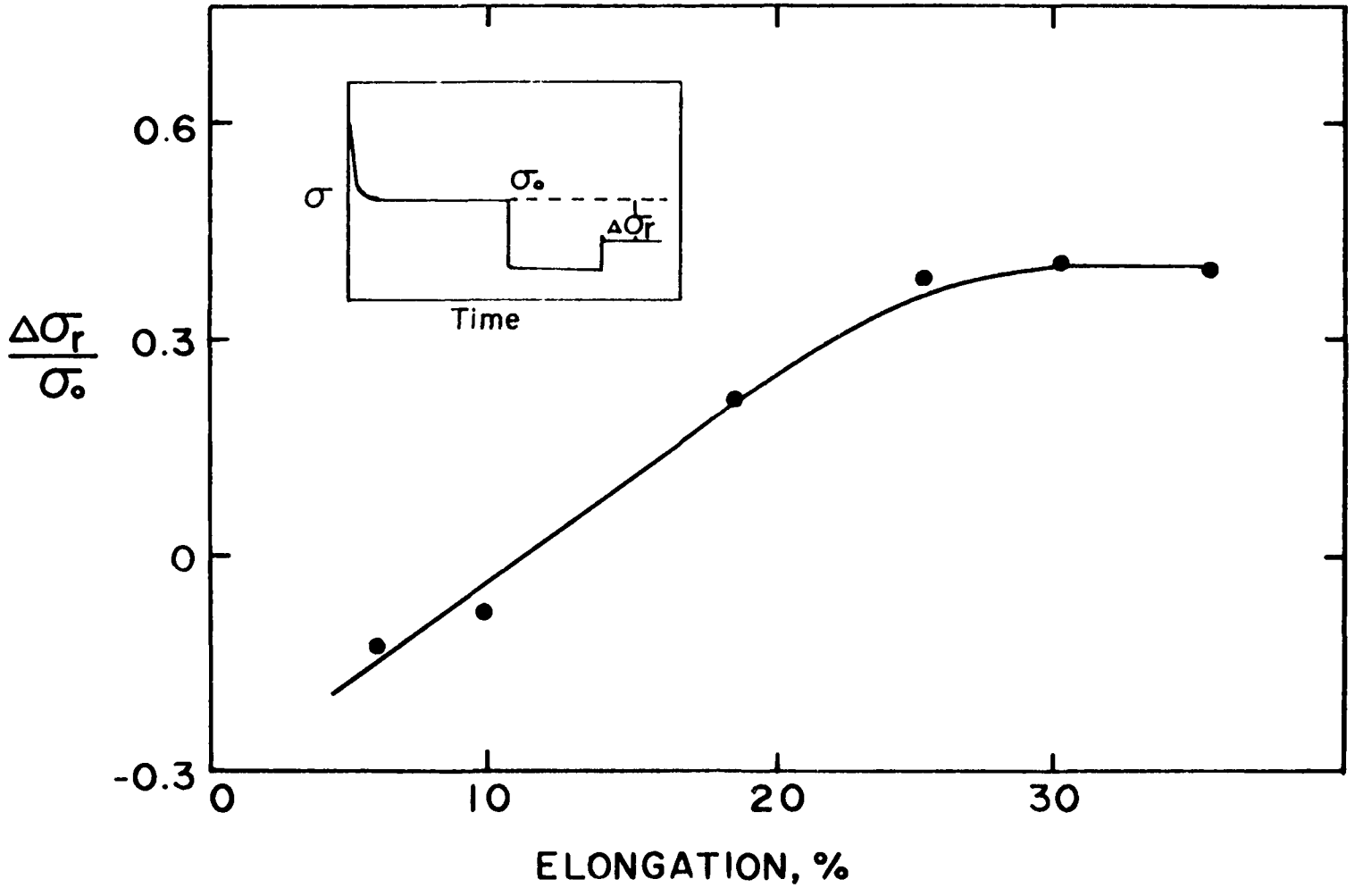
0.6
0.3
0
-0.3
$\frac{\Delta\sigma_r}{\sigma_o}$
σ
σ_o
$\Delta\sigma_r$
Time
0
10
20
30
ELONGATION, %

FIGURE 9

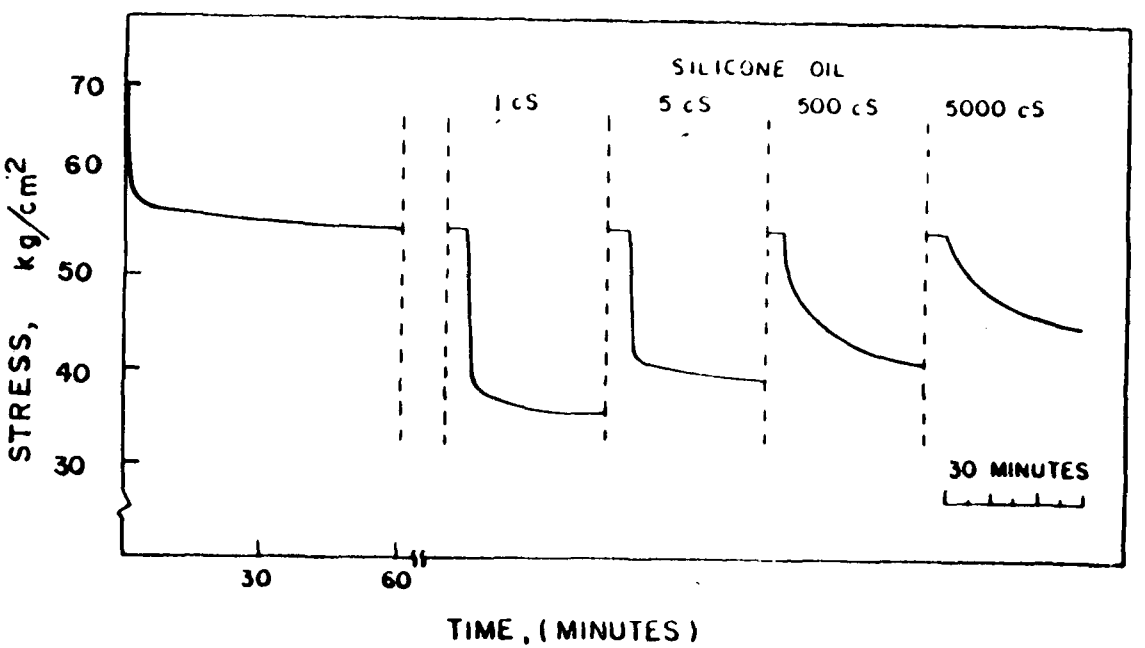
SILICONE OIL
1 cS
5 cS
500 cS
5000 cS
70
60
50
40
30
STRESS, kg/cm²
30 MINUTES
30
60
TIME, (MINUTES)

FIGURE 10

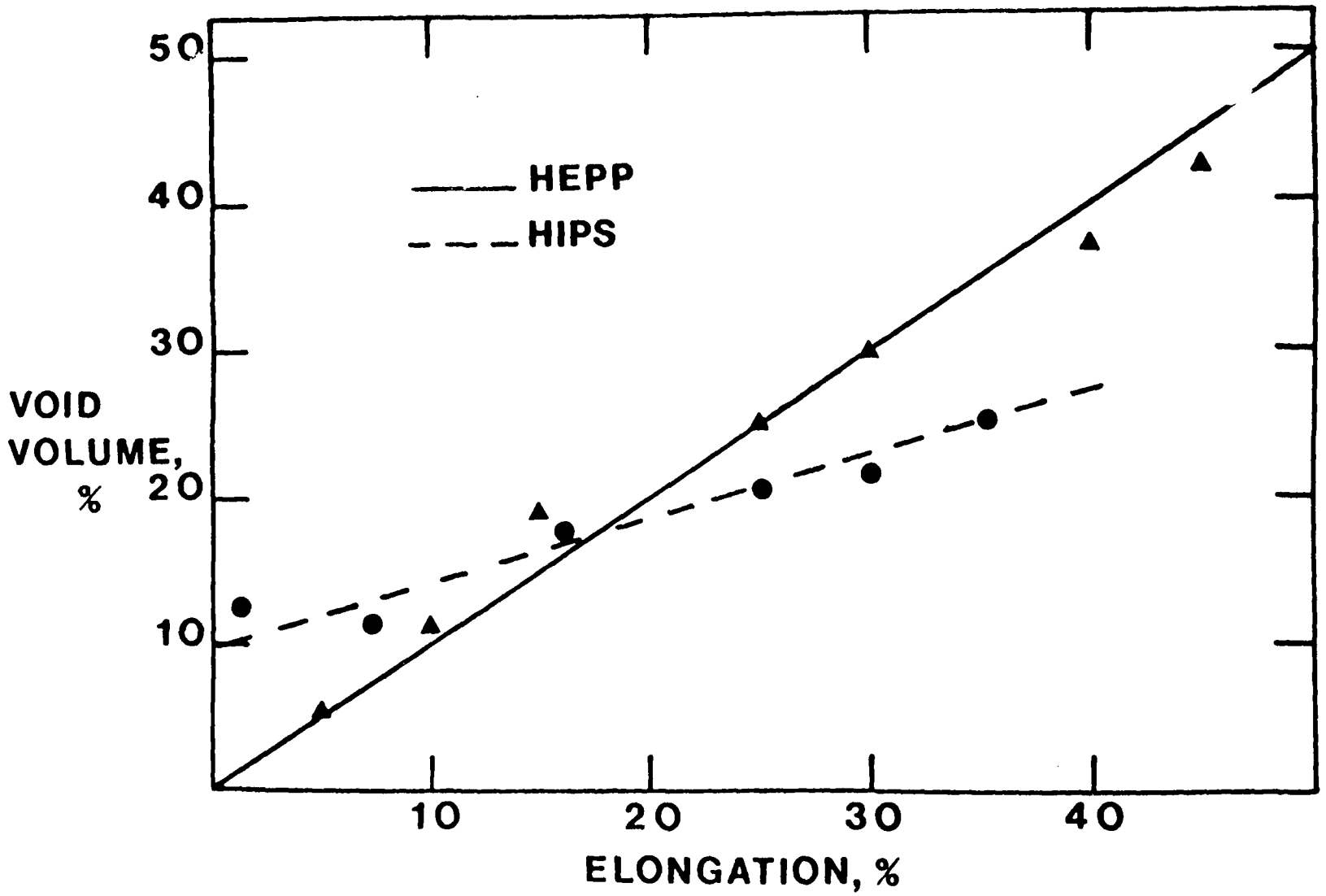

FIGURE 11

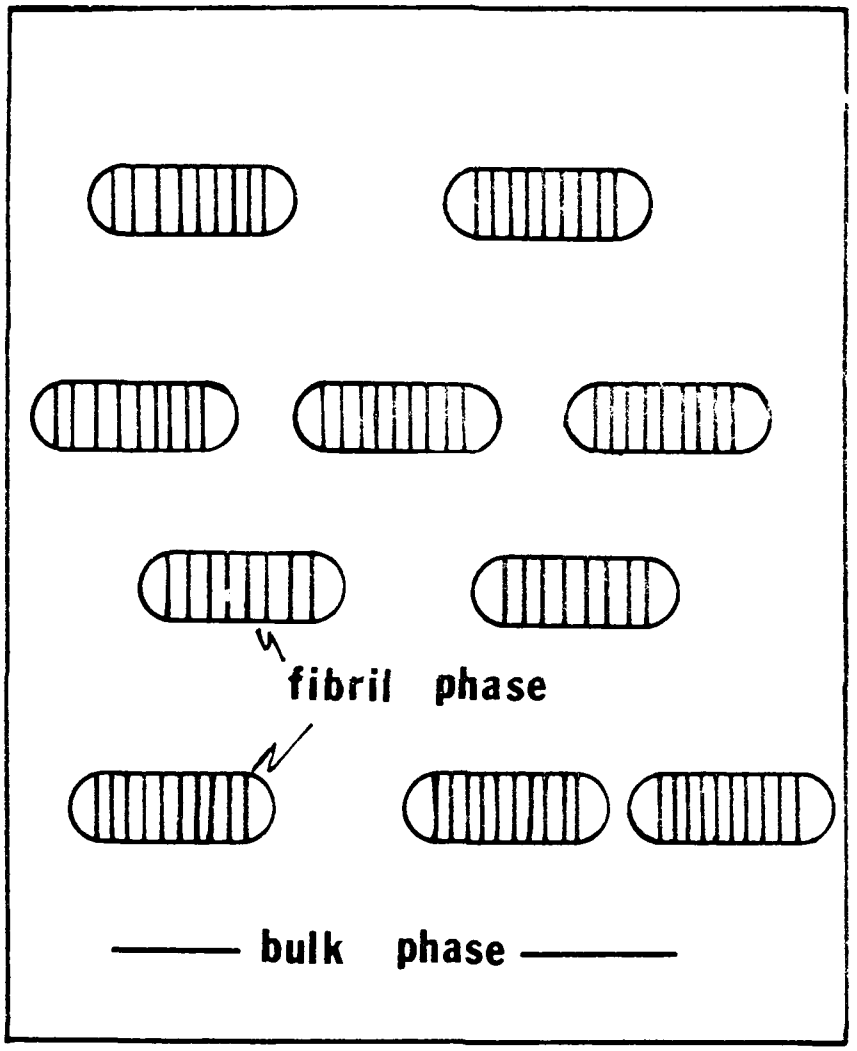

Figure 12

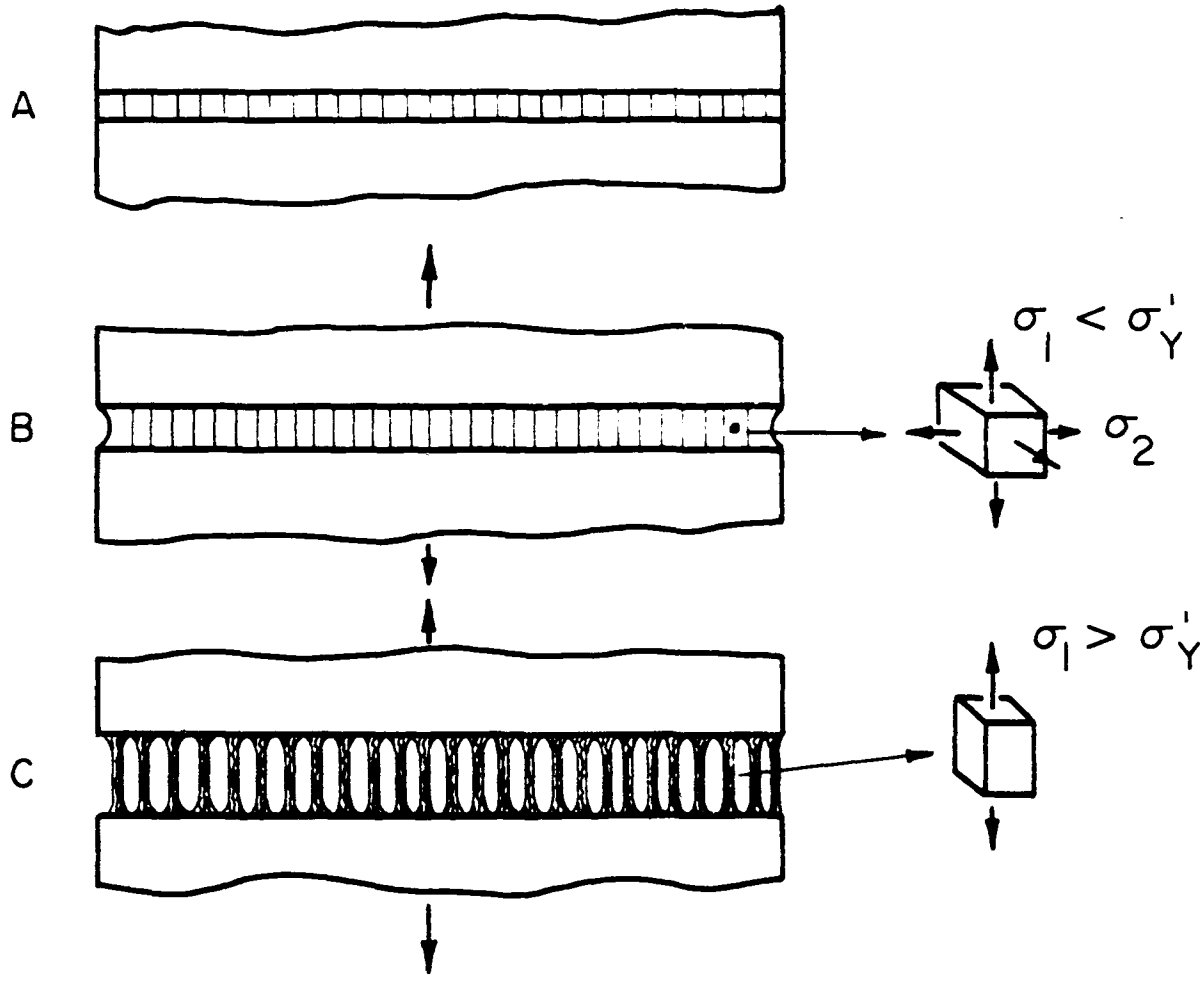

Figure 13

$\sigma_1 < \sigma_Y'$

σ_2

$\sigma_1 > \sigma_Y'$

END

DATE
FILMED

10-8

DTIC